30th Annual International IEEE EMBS Conference
Vancouver, British Columbia, Canada, August 20-24, 2008

Specular surface reconstruction for multi-camera corneal topographer arrangements

Zoltán Fazekas, Alexandros Soumelidis, András Bódis-Szomorú and Ferenc Schipp

Abstract— **A novel specular surface reconstruction approach developed for and used in an experimental multi-camera corneal topographer arrangement is presented in the paper. The tear-film coated, and therefore specular, corneal surface is mathematically reconstructed from the corneal images taken simultaneously by the calibrated cameras of the arrangement. The surface reconstruction is achieved by the joint solution of partial differential equations (PDE's) that is derived from the mapping between the measurement-pattern and its virtual images taken by the cameras. The PDE's – each given in an advantageous form for one of the cameras – describe the phenomenon of light-reflection at the corneal surface. The portions of the corneal surface that reflect – possibly different – measurement-pattern points to more than one camera convey starting points for the mathematical reconstruction of the surface.**

I. INTRODUCTION

The outer shape – i.e., the outer surface – of the human cornea generates about the 70% of the total refractive power of the human eye. It is mainly for this reason that the detailed topographic characterization of the corneal surface has considerable diagnostic value. Examination devices and methods aiming at determining the corneal shape – and using it for further optical calculations – have a relatively long history [3] in ophthalmology. Today, corneal topographers are used in a wide range of ophthalmic examinations [2]. The majority of the measurement methods used in corneal topographers rely on the specularity of the cornea, or more precisely, that of the pre-corneal tear-film. These methods are referred as reflection-based methods, and the topographers using these methods as reflection-based topographers. In case of such topographers, a bright measurement-pattern of known and well-defined geometry – e.g., concentric rings called in this context Placido-rings – is generated and displayed in front of the patient's cornea. The reflection of this pattern at the pre-corneal tear-film is photographed by one or more camera. The distorted virtual image, or images are then analyzed, and the corneal surface is mathematically reconstructed. Based on this reconstruction, height- and refractive power-maps are produced and displayed for inspection by the ophthalmologist. In case of healthy and regular corneal surfaces, the presently available corneal topographers generally produce good quality corneal snapshots, and based on these, precise and reliable maps are generated. However, even for healthy regular surfaces, small impurities and tiny discontinuities in the pre-corneal tear-film may produce extensive measurement errors. It is particularly the case, when simplistic measurement-patterns, such as the one mentioned above, are used. To this end, several more informative measurement-patterns were suggested recently. These patterns facilitate the identification of point-correspondences by using location-dependent color-coding, e.g., [10].

This research has been partially supported by the National Office for Research and Technology (NORT), Hungary, in the frame of the NKFP-2/020/04 research contract.

A. Soumelidis and Z. Fazekas are with the Computer and Automation Research Institute (SZTAKI) Budapest, Hungary, {soumelidis,zfazekas}@sztaki.hu

A. Bódis-Szomorú is with the Department of Measurement and Information Systems, Budapesti University of Technology and Economics, Budapest, Hungary, bodis@mit.bme.hu

F. Schipp is with the Department of Numerical Analysis, Eötvös Loránd University, Budapest, Hungary, schipp@ludens.elte.hu

II. RECONSTRUCTION OF SMOOTH SPECULAR SURFACES

The mathematical reconstruction of smooth specular surfaces from the distortion they cause to some known pattern – when the pattern is viewed, or photographed as being reflected from the mentioned surface – is an active research area. The reconstruction can be local or global.

In case of local reconstruction, sufficient conditions are given for the uniqueness of a local surface reconstructions in [6]. Also, the formulae to determine the actual surface-patch are given there.

A. Global reconstruction.

Methods for the practically more important global reconstruction are published in [7], [9]. Each of these methods relies on the smoothness of the surface to be reconstructed and uses several views to make the unique reconstruction possible. For an unknown smooth, convex specular surface – viewed by several cameras – those points are located on or near to the specular surface for which the unit normal vectors – calculated from the real or assumed reflections at these points – are approximately the same for different views. This observation is the basis of the voxel-carving method suggested by [7]. Clearly, this method can be used only for those surface portions that reflect the measurement-pattern into more than one camera. An elegant surface reconstruction method was proposed by [9]. There the light-reflection at the surface is described with a total differential equation. The mathematical reconstruction of the surface is achieved by the numerical solution of the aforementioned differential equation.

III. THE PROPOSED RECONSTRUCTION METHOD

A. The multi-camera arrangement.

The surface reconstruction method proposed in the present paper was developed for an experimental corneal topographer

arrangement – referred as target-arrangement – comprising up to four cameras. The target-arrangement and its hardware were described in detail in [10]. A three-camera version of such an arrangement is shown in Fig. 1. It should be underlined that the surface reconstruction method derived for the target-arrangement is applicable to most multi-camera arrangements that are reasonable in the given application. Here, only a brief description of the target-arrangement is included, its sole purpose is to provide a context for the proposed surface reconstruction method. The target-arrangement comprises a TFT-display for displaying a measurement-pattern. Furthermore, it comprises three color-cameras which are rigidly mounted on the display. Each camera is aimed at the patient's eye. For the reconstructions presented herein, a rectangular array of bright circular spots was used as measurement-pattern. It is discernible in the mentioned figure.

B. Image segmentation and filtering.

The reflected blobs – corresponding to the circular spots in the rectangular array of the measurement-pattern – were detected at a number of thresholds, and the center-point and a few shape-descriptors were calculated for each blob. The blobs were then checked for their areas, axis-lengths and their orientation. Blobs being relatively close to each other and having similar shape-descriptor values were united, as these were assumed to be the images of the same circular spot. Blobs with much bigger areas than those of the nearby blobs were removed, as these were assumed to be segmentation artifacts. The blob-centers resulting from the above process can be seen in Fig. 2 for an artificial cornea.

C. Blob identification.

A colored spot was used for marking the center of the rectangular array. The corresponding blobs in the three reflection images were identified firstly and their center-points were used as reference and starting points for the subsequent blob-identification process. Each of the three 2D-point-sets – formed by the blob-centers of the blobs detected in the reflection images – were submitted to Delaunnay-triangulation. The sides of the resulting triangles were then tracked – starting from the aforementioned reference points – in "row" and "column" directions. A "row" curve and a "column" curve – corresponding to a particular row and column in the measurement-pattern – are shown in Fig. 2. Based on the tracking results, correspondences (i.e., mapping) between the original circular spots on one hand and the detected blobs on the other were then established.

Fig. 1. A patient's eye is photographed with a three-camera corneal topographer arrangement.

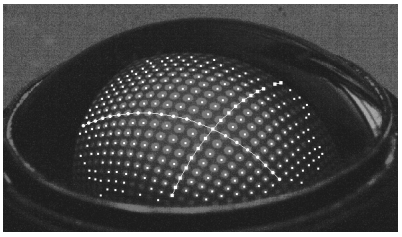

Fig. 2. The detected blobs – with their center-points marked – in case of an artificial cornea.

For the purpose of the tracking the side-lengths of the Delaunnay-triangles, the directions of sides and the area-ratio of the blobs concerned were used. In Fig. 3, the blob-area – shown as height – for each blob-center detected is displayed for the spherical artificial cornea shown in Fig. 2. For the 2D point-set – formed by the blob-centers – a 2D Delaunnay-triangulation was carried out and the resulting triangular mesh is shown on the surface.

D. Approximation of the apparent distortions.

Spline interpolation was used to convert the aforementioned discrete mappings – that is, the mappings between the original spot-centers and the blob-centers detected in the reflection images – to continuous mappings, thereby approximating the optical mappings (distortions) between the points of the measurement-pattern and those of the reflection images. Such a spline interpolation is shown for a particular "row" and a "column" in Fig. 2 for an artificial cornea. A mesh of splines is shown for a corneal surface in Fig. 8.

E. Mathematical model of the light-reflection at the specular surface.

Mathematically, the smooth specular convex surface F is described and sought in preferably chosen spatial coordinate systems. Each of these coordinate systems corresponds to one of the cameras of the topographer arrangement. For

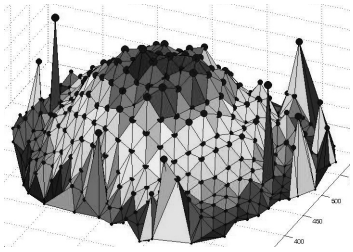

Fig. 3. The blob-areas of the blobs detected in the reflection image shown in Fig. 2

notational simplicity, only one of these coordinate system is considered in the following formulae.

The origin of the camera coordinate system B is placed in the optical center of the particular camera and the z-axis of this coordinate system is the optical axis BB' of the camera. The specular surface F – i.e., the surface of an artificial or a real cornea – is described in the following form:

$$F(x_1, x_2) = S(x_1, x_2)\hat{x} \qquad (\hat{x} = (x_1, x_2, 1)^T) \qquad (1)$$

Here, $S(x)$ $(x = (x_1, x_2))$ is a scalar-factor describing the inverse distance-ratio, measured from B, of the 3D point P_x – corresponding to $\hat{x}$ – and the surface-point appearing in the same direction as P_x from B. The propagation of light from the points of the measurement pattern to those of the (distorted) image, i.e., $P_y P P_x$, is described in the coordinate system. By doing so, a mapping is identified between the points P_y of the measurement pattern and the points P_x of the image: $P_y \rightarrow P_x$. It follows from the conditions prescribed for the mathematical surface that mapping $P_y \rightarrow P_x$ is one-to-one. It follows from the physical law of light-reflection, the two-variable function $S(x)$ describing surface F satisfies the following first-order partial differential equation (PDE):

$$\frac{1}{S(x)} \frac{\partial S(x)}{\partial x_j} = \frac{v_j(x) - x_j}{\langle \hat{x}, \hat{x} - v(x) \rangle} \qquad (j = 1, 2), \qquad (2)$$

where

$$v(x) = |\hat{x}\,| \frac{k + f(x) - S(x)\hat{x}}{|k + f(x) - S(x)\hat{x}|} \quad ,$$

and function $f(x)$ can be expressed with the inverse of $P_y \rightarrow P_x$ mapping, i.e., with mapping $P_x \rightarrow P_y$. In (2), k is a vector pointing to a reference point in the plane of the measurement pattern; while $\langle ., . \rangle$ denotes the scalar product of the 3D space. It follows from the mathematical model described above that surface F can be determined uniquely under the starting condition of $S(0, 0) = s_0$, if the $P_y \rightarrow P_x$ mapping is known.

F. Using stereo information for determining the starting condition.

The exact value of the above starting condition could be found out by including two laser-lights for each camera (as done in other topographers). However, this distance setting mechanism is unnecessary here, as precise stereo information can be gathered with two calibrated cameras looking at the same patch of specular surface.

An assumed surface-point and the its corresponding unit normal vector – determined from the first reflection image, or more precisely from the first mapping – are used to determine the point in the measurement-pattern that should be seen in the second image. The Euclidean distance between the point determined in this manner and the point in the measurement-pattern that is really seen by the second camera is calculated. The presence of such an error indicates for an assumed surface-point that it is – in reality – off the surface. By moving along possible surface-points – and considering also their derived unit normal vectors – that are viable for the first camera, the aforementioned error must be minimized. The near-zero valued minima mark the spatial positions of some surface-points that can be used as stating points.

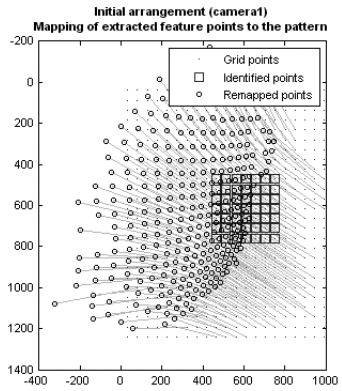

Fig. 4. Fine-tuning the calibration.

G. Individual and joint camera calibration.

In the procedure outlined in Section III-F that determines the starting condition for the PDE given in Section III-E, it was tacitly assumed that the cameras were calibrated. To satisfy this assumption, the chessboard-based calibration approach described in [4] was used. A free MATLAB-implementation is available on the web and is described in [11]. This implementation, however, is difficult to handle, and useful restrictions on camera-parameters cannot be easily imposed. For these reasons, a new implementation of the above calibration approach was developed and used.

A 10mm*10mm chessboard was used as calibration object. Firstly, it was placed in an approximately vertical position and was photographed, then the chessboard was fixed onto a wedge and was turned around an axis more or less perpendicular to the measurement-pattern's plane. The chessboard was photographed in a number of positions, then the above camera calibration procedure was carried out for each camera. The plane-positions recovered in the calibration process were as expected, and so were indicating a good calibration precision.

However, it soon turned out that the calibration of the multi-camera arrangement – based on these individual camera calibrations only – does not ensure the precision needed for surface reconstruction. Therefore, a second – fine-tuning – calibration step was necessary; a joint calibration of the

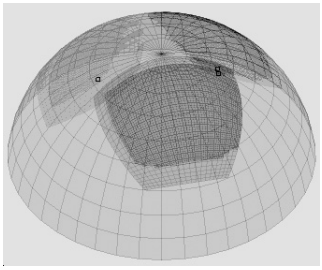

Fig. 5. The reconstructed surface of the artificial cornea shown in Fig. 2.

Fig. 6. The measurement pattern reflected in an eye.

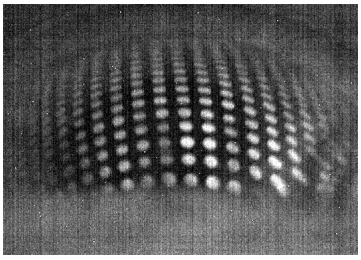

Fig. 7. One of the reflection images.

cameras in the topographer arrangement was carried out. The simulation programs developed for modeling reflections of smooth specular surfaces turned out handy for this purpose. A spherical artificial cornea with know radius was used as a calibration object.

An optimization procedure was carried out with respect to the position of the artificial cornea and the external camera-parameters of the cameras in the arrangement, the aim was to minimize the total sum of quadratic error between the blob-centers in the simulated reflection images and the detected ones.

The effect – in point-positions in the measurement-pattern's plane – of this optimization is shown in Fig. 4. The resulting "flow" is clearly visible and quite dramatic.

H. The surface reconstruction procedure.

A numerical procedure taking discrete values of the mapping as input was devised to calculate the $P_x \rightarrow P_y$ mapping. As mentioned in Section III-D relies on spline interpolation.

Furthermore, a numerical procedure was devised to solve the PDE's given in Section III-E. The solution of these PDE's in effect conveys the reconstructed surface. The solution of the PDE's involved their transcriptions for "row" and "column" directions. In this manner, first-order ordinary non-linear differential equations were generated. These were then numerically integrated – using the well-known Runge-Kutta method – along "row" and "column" directions, as necessary.

The starting conditions were derived with the method outlined in Section III-F. A computational scheme was devised to re-use the points computed earlier to improve reconstruction speed. In Figs. 6, 7, 8 and 9, the main stages of the reconstruction process can be followed for a living cornea.

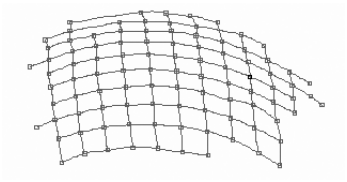

Fig. 8. Spline interpolation between the detected blob-centers.

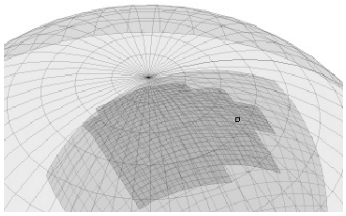

Fig. 9. A surface region reconstructed from one of the camera-views.

IV. CONCLUSION AND FUTURE WORKS

The majority of the topographers in use today, rely on one view only, which is theoretically insufficient for the unique reconstruction of the corneal surface. To overcome this essential measurement deficiency, a multi-camera arrangement was proposed earlier by the authors and mathematical methods were devised for surface reconstruction. Clearly, further experimentation and simulations are required to improve the multi-camera arrangement. With an improved arrangement, it will be easier to produce images with good overlapping.

REFERENCES

[1] M.A. Halstead, B.A. Barsky, S.A. Klein and R.B. Mandell, "Reconstructing curved surfaces from specular reflection patterns using spline surface fitting to normals", *in ACM SIGGRAPH*, ACM, 1996.

[2] M.C. Corbett, E.S. Rosen and D.P.S. O'Brart, *Corneal topography: principles and practice*, Bmj Publ. Group, London, UK, 1999.

[3] F. Jongsma, J. de Brabander and F. Hendrikse, Review and classification of corneal topographers. *Lasers in Medical Science*, vol. 14, 1999, pp 2-19.

[4] Z. Zhang, A flexible new technique for camera calibration, *IEEE Transactions on Pattern Analysis and Machine Intelligence*, vol. 22, no. 11, 2000, pp 1330-1334.

[5] S. Savarese, M. Chen and P. Perona, "Second order local analysis for 3d reconstruction of specular surfaces", in *Proceedings of the First International Symposium on 3D Data Processing Visualisation and Transmission*, IEEE, 2002.

[6] S. Savarese and P. Perona, "Local analysis for 3d reconstruction of specular surfaces - part ii", in Lecture Notes In Computer Science, vol. 2351, *Proceedings of the 7th European Conference on Computer Vision*, Springer-Verlag, 2002.

[7] T. Bonfort and P. Sturm, "Voxel carving for specular surfaces", in *9th IEEE Conference on Computer Vision*, vol. 2, 2003

[8] S. Savarese, M. Chen and P. Perona, "What do reflections tell us about the shape of a mirror?" in *Applied Perception in Graphics and Visualization*, ACM SIGGRAPH, ACM, 2004.

[9] R. Kickingereder and K. Donner, "Stereo vision on specular surfaces", *in Proceedings of the 4th IASTED International Conference on Visualization, Imaging, and Image Processing*, IASTED, 2004.

[10] A. Soumelidis, Z. Fazekas, F. Schipp, A. Edelmayer, J. Németh and B. Csákány, "Development of a multi-camera corneal topographer using an embedded computing approach", in *Proceedings of the First International Conference on Biomedical Electronics and Devices*, Funchal, Madeira, Portugal, 2008, pp 126-129.

[11] J.-Y. Bouguet, *Camera Calibration Toolbox for MATLAB*, California Institute of Technology, 2007.